

Widely tunable single photon source with high purity at telecom wavelength

Rui-Bo Jin,^{1,*} Ryosuke Shimizu,² Kentaro Wakui,¹ Hugo Benichi,¹ and Masahide Sasaki¹

¹National Institute of Information and Communications Technology, 4-2-1 Nukui-Kitamachi, Koganei, Tokyo 184-8795, Japan

²Center for Frontier Science and Engineering, University of Electro-Communications, 1-5-1 Chofugaoka, Chofu, Tokyo 182-8585, Japan

*ruibo@nict.go.jp

Abstract: We theoretically and experimentally investigate the spectral tunability and purity of photon pairs generated from spontaneous parametric down conversion in periodically poled KTiOPO₄ crystal with group-velocity matching condition. The numerical simulation predicts that the purity of joint spectral intensity (P_{JSI}) and the purity of joint spectral amplitude (P_{JSA}) can be kept higher than 0.98 and 0.81, respectively, when the wavelength is tuned from 1460 nm to 1675 nm, which covers the S-, C-, L-, and U-band in telecommunication wavelengths. We also directly measured the joint spectral intensity at 1565 nm, 1584 nm and 1565 nm, yielding P_{JSI} of 0.989, 0.983 and 0.958, respectively. Such a photon source is useful for quantum information and communication systems.

© 2018 Optical Society of America

OCIS codes: (270.0270) Quantum optics; (190.4410) Nonlinear optics, parametric processes; (270.5585) Quantum information and processing; (270.5565) Quantum communications.

References and links

1. F. J. Duarte, ed., *Tunable Laser Applications* (CRC Press, 2008), 2nd ed.
2. R. Paschotta, *Encyclopedia of Laser Physics and Technology* (Wiley-VCH, 2008).
3. T. B. Hoang, J. Beetz, M. Lerner, L. Midolo, M. Kamp, S. Höling, and A. Fiore, “Widely tunable, efficient on-chip single photon sources at telecommunication wavelengths,” *Opt. Express* **20**, 21758–21765 (2012).
4. M. Benyoucef, H. S. Lee, J. Gabel, T. W. Kim, H. L. Park, A. Rastelli, and O. G. Schmidt, “Wavelength tunable triggered single-photon source from a single cdt quantum dot on silicon substrate,” *Nano Letters* **9**, 304–307 (2009).
5. T. E. Keller and M. H. Rubin, “Theory of two-photon entanglement for spontaneous parametric down-conversion driven by a narrow pump pulse,” *Phys. Rev. A* **56**, 1534–1541 (1997).
6. W. P. Grice and I. A. Walmsley, “Spectral information and distinguishability in type-II down-conversion with a broadband pump,” *Phys. Rev. A* **56**, 1627–1634 (1997).
7. F. König and F. N. C. Wong, “Extended phase matching of second-harmonic generation in periodically poled KTiOPO₄ with zero group-velocity mismatch,” *Appl. Phys. Lett.* **84**, 1644–1646 (2004).
8. P. G. Evans, R. S. Bennink, W. P. Grice, T. S. Humble, and J. Schaake, “Bright source of spectrally uncorrelated polarization-entangled photons with nearly single-mode emission,” *Phys. Rev. Lett.* **105**, 253601 (2010).
9. A. Eckstein, A. Christ, P. J. Mosley, and C. Silberhorn, “Highly efficient single-pass source of pulsed single-mode twin beams of light,” *Phys. Rev. Lett.* **106**, 013603 (2011).
10. M. Yabuno, R. Shimizu, Y. Mitsumori, H. Kosaka, and K. Edamatsu, “Four-photon quantum interferometry at a telecom wavelength,” *Phys. Rev. A* **86**, 010302 (2012).
11. P. J. Mosley, J. S. Lundeen, B. J. Smith, and I. A. Walmsley, “Conditional preparation of single photons using parametric downconversion: a recipe for purity,” *New Journal of Physics* **10**, 093011 (2008).
12. K. Edamatsu, R. Shimizu, W. Ueno, R.-B. Jin, F. Kaneda, M. Yabuno, H. Suzuki, S. Nagano, A. Syouji, and K. Suizu, “Photon pair sources with controlled frequency correlation,” *Progress in Informatics* **8**, 19–26 (2011).

13. A. B. U'Ren, C. Silberhorn, K. Banaszek, I. A. Walmsley, R. Erdmann, W. P. Grice, and M. G. Raymer, "Generation of pure-state single-photon wavepackets by conditional preparation based on spontaneous parametric downconversion," *Laser Physics* **15**, 146–161 (2005).
14. J. Eberly, "Schmidt analysis of pure-state entanglement," *Laser Physics* **16**, 921–926 (2006).
15. A. M. Brańczyk, A. Fedrizzi, T. M. Stace, T. C. Ralph, and A. G. White, "Engineered optical nonlinearity for quantum light sources," *Opt. Express* **19**, 55–65 (2011).
16. M. Fiorentino and R. G. Beausoleil, "Compact sources of polarization-entangled photons," *Opt. Express* **16**, 20149–20156 (2008).
17. A. Fedrizzi, T. Herbst, A. Poppe, T. Jennewein, and A. Zeilinger, "A wavelength-tunable fiber-coupled source of narrowband entangled photons," *Opt. Express* **15**, 15377–15386 (2007).
18. A. Predojević, S. Grabher, and G. Weihs, "Pulsed sagnac source of polarization entangled photon pairs," *Opt. Express* **20**, 25022–25029 (2012).
19. T. Gerrits, M. J. Stevens, B. Baek, B. Calkins, A. Lita, S. Glancy, E. Knill, S. W. Nam, R. P. Mirin, R. H. Hadfield, R. S. Bennink, W. P. Grice, S. Dorenbos, T. Zijlstra, T. Klapwijk, and V. Zwiller, "Generation of degenerate, factorizable, pulsed squeezed light at telecom wavelengths," *Opt. Express* **19**, 24434–24447 (2011).

1. Introduction

As it is well known, classical widely tunable laser sources play an important role in many fields, for example, spectroscopy, remote sensing, metrology, and optical communications [1, 2]. However, the quantum counterpart of the tunable laser, the widely tunable single photon source, have been less investigated. Wavelength tunable single photon sources have been generated from quantum dots, but the tunable ranges achieved until now have been narrow [3, 4].

In this paper, we present a widely tunable single photon source based on spontaneous parametric down conversion (SPDC) in a periodically poled KTiOPO_4 (PPKTP) crystal with group-velocity matching condition. The concept of group-velocity matching in SPDC was introduced by Keller and Rubin [5], and by Grice and Walmsley [6] in 1997. PPKTP crystal with group-velocity matching condition was experimentally demonstrated by König and Wong [7] for second-harmonic generation in 2004. Later, this condition was applied in SPDC for intrinsically pure photon state generation. Under this condition, the signal and idler photons from SPDC have no spectral correlation, *i.e.*, they are intrinsically pure. Therefore, there is no need to employ bandpass filters to obtain high-purity heralded single photons. Consequently, such photon sources are much brighter than the traditional sources and have showed high brightness in experiments, as reported by Evans, *et al.*, for entangled photons [8]; by Eckstein, *et al.*, for two-mode squeezer [9]; and by Yabuno, *et al.*, for four-photon interferometry [10].

Besides the high purity and high brightness, in this research, we focus on another important merit of this source: the wide spectral tunability. From the numerical calculation, we found that the purity of joint spectral intensity (P_{JSI}) and the purity of joint spectral amplitude (P_{JSA}) can be kept higher than 0.98 and 0.81, respectively, as the wavelength is tuned from 1460 nm to 1675 nm. To verify this simulation, we directly measured the joint spectral intensity, and obtained high P_{JSI} of 0.989, 0.983 and 0.958 at 1565 nm, 1584 nm and 1565 nm, respectively.

2. Theory

In the process of SPDC, one pump photon is split into two lower energy photons, the signal and the idler. The two-photon component in SPDC can be expressed as [11]

$$|\Psi_{si}\rangle = \int_0^\infty \int_0^\infty d\omega_s d\omega_i f(\omega_s, \omega_i) \hat{a}_s^\dagger(\omega_s) \hat{a}_i^\dagger(\omega_i) |0\rangle, \quad (1)$$

where $f(\omega_s, \omega_i) = \phi(\omega_s, \omega_i)\alpha(\omega_s + \omega_i)$ is the joint spectral amplitude (JSA), $\phi(\omega_s, \omega_i)$ and $\alpha(\omega_s + \omega_i)$ are the phase matching amplitude and the pump envelope amplitude. ω is the angular frequency, \hat{a}^\dagger is the creation operator and the subscripts s and i denote the signal

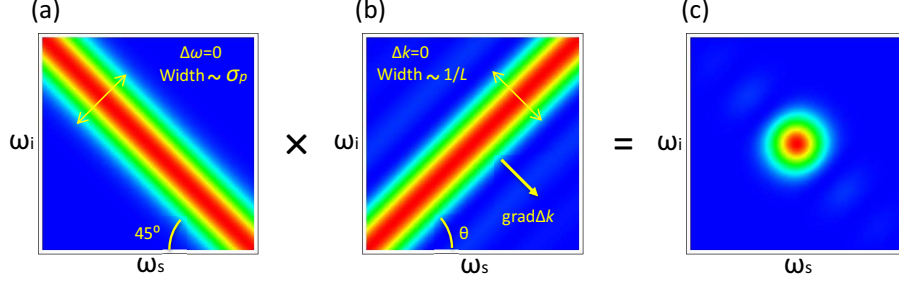


Fig. 1. Examples of (a) pump envelope intensity (PEI), (b) phase matching intensity (PMI) and (c) joint spectral intensity (JSI). (c) is the product of (a) and (b). The width of PEI is proportional to the bandwidth of the pump, while the tilting angle of PEI is fixed, 45 degree to the minus direction of the horizontal axis. The width of PMI is proportional to the inverse of the crystal length. The direction of PMI is not fixed, but determined by the group velocities of the signal, the idler and the pump. When the width of PEI and PMI are equal and the PMI is at 45 degree to the positive direction of the horizontal axis, JSI can achieve a subcircular shape and maximum purity.

and the idler photons, respectively. Assuming the spectrum of the pump laser has a Gaussian distribution with a bandwidth of σ_p , the pump envelope intensity can be written as $|\alpha(\omega_s + \omega_i)|^2 = \exp[-(\frac{\omega_s + \omega_i - \omega_p}{\sigma_p})^2]$. Under the collinear condition, the phase matching intensity can be written in the form of $|\phi(\omega_s, \omega_i)|^2 = [\text{sinc}(\frac{\Delta k L}{2})]^2$, where $\Delta k = k_p - k_s - k_i - \frac{2\pi}{\Lambda}$ is the difference between the wave vector of the pump (k_p), the signal (k_s), the idler (k_i) and an extra vector ($\frac{2\pi}{\Lambda}$) introduced by periodical poling of the crystal. L and Λ are the length and poling period of the SPDC crystal. Figure 1(a-c) shows examples of the pump envelope intensity $|\alpha(\omega_s + \omega_i)|^2$, phase matching intensity $|\phi(\omega_s, \omega_i)|^2$ and joint spectral intensity (JSI) $|f(\omega_s, \omega_i)|^2$.

Considering the Taylor expansion of the three wave vectors $k_\mu = k_\mu(\omega_{\mu 0}) + k'_\mu(\omega_{\mu 0})(\omega_\mu - \omega_{\mu 0}) + o((\omega_\mu - \omega_{\mu 0})^2)$, ($\mu = p, s, i$), the difference of them can be approximated as $\Delta k = \Delta k^{(0)} + \Delta k^{(1)} + \dots$. In our experiment, the phase matching condition is satisfied at $\omega_s = \omega_i = \omega_0 = \frac{\omega_p}{2}$ and thus the zero order contribution disappears:

$$\Delta k^{(0)} = k_p(2\omega_0) - k_s(\omega_0) - k_i(\omega_0) - \frac{2\pi}{\Lambda} = 0. \quad (2)$$

The first order term can be written as

$$\begin{aligned} \Delta k^{(1)} &= k'_p(2\omega_0)(\omega_p - 2\omega_0) - k'_s(\omega_0)(\omega_s - \omega_0) - k'_i(\omega_0)(\omega_i - \omega_0) \\ &= [k'_p(2\omega_0) - k'_s(\omega_0)](\omega_s - \omega_0) + [k'_p(2\omega_0) - k'_i(\omega_0)](\omega_i - \omega_0), \end{aligned} \quad (3)$$

where “ \prime ” represents the first order differentiation with respect to the angular frequency.

As analyzed in [12], the slope of the phase matching condition is determined by the gradient of Δk .

$$\mathbf{grad}\Delta k = (\frac{\partial \Delta k}{\partial \omega_s}, \frac{\partial \Delta k}{\partial \omega_i}) = (V_{g,p}^{-1}(\omega_p) - V_{g,s}^{-1}(\omega_s), V_{g,p}^{-1}(\omega_p) - V_{g,i}^{-1}(\omega_i)), \quad (4)$$

where the group velocity $V_{g,\mu}$ is defined as $V_{g,\mu} = \frac{d\omega}{dk_\mu(\omega)} = \frac{1}{k'_\mu(\omega)}$, ($\mu = p, s, i$). From the viewpoint of the tilting angle, θ ,

$$\tan\theta = -\frac{V_{g,p}^{-1}(\omega_p) - V_{g,s}^{-1}(\omega_s)}{V_{g,p}^{-1}(\omega_p) - V_{g,i}^{-1}(\omega_i)}, \quad (5)$$

where θ is the angle between positive direction of horizontal axis and the ridge direction of the phase matching intensity, as shown in Fig. 1(b).

The purity, a parameter which describes the spectral correlation of the photon source, is defined as $p = \text{Tr}(\hat{\rho}_s^2) = \text{Tr}(\hat{\rho}_i^2)$, where $\hat{\rho}_s = \text{Tr}_i(|\psi_{si}\rangle\langle\psi_{si}|)$ is the reduced density operator of the signal, and Tr_i represents the partial trace on the subsystem i . This purity is determined by the factorability of the JSA, $f(\omega_s, \omega_i)$, and can be calculated numerically using Schmidt decomposition [11, 13]. By applying Schmidt decomposition on the JSA, we can obtain

$$f(\omega_1, \omega_2) = \sum_j c_j \phi_j(\omega_1) \varphi_j(\omega_2), \quad (6)$$

where $\phi_j(\omega_1)$ and $\varphi_j(\omega_2)$ are two orthogonal basis sets of spectral functions, known as the Schmidt modes. c_j is a set of real, non-negative, normalized weighting coefficients with $\sum_j c_j^2 = 1$. The Schmidt number is defined as $K = \frac{1}{\sum_j c_j^4}$ [14]. K indicates the number of Schmidt modes existing in the two-photon state and thus can be viewed as an indicator of entanglement. The purity of the signal or the idler state equals to the inverse of the Schmidt number K :

$$p = P_{JSA} = \sum_j c_j^4. \quad (7)$$

In experiment, it is difficult to directly measure $f(\omega_1, \omega_2)$, the JSA. What we usually measured is $|f(\omega_s, \omega_i)|^2$, the JSI, as have been widely demonstrated in previous experiments [8, 9, 10, 11]. To analyze such experimental data in experiment, the Schmidt decomposition can be applied on $|f(\omega_s, \omega_i)|^2$,

$$|f(\omega_1, \omega_2)|^2 = \sum_j c_j^2 \phi_j(\omega_1) \varphi_j(\omega_2). \quad (8)$$

We define the purity of the joint spectral intensity as

$$P_{JSI} = \sum_j c_j^4. \quad (9)$$

P_{JSI} is useful in experiment to characterize the joint spectral intensity. In this paper we focus on the parameter P_{JSI} .

3. Numerical simulation

With the Sellmeier equation in [7], we calculated P_{JSI} and P_{JSA} versus the wavelength, as shown in Fig. 2. The horizontal axis is the wavelength of the signal (or the idler, in degenerate case), which is two times of the pump wavelength. The bandwidth of the pump is set to match the length of the crystal, so as to achieve the maximum purity at 1584 nm. The optimal bandwidths

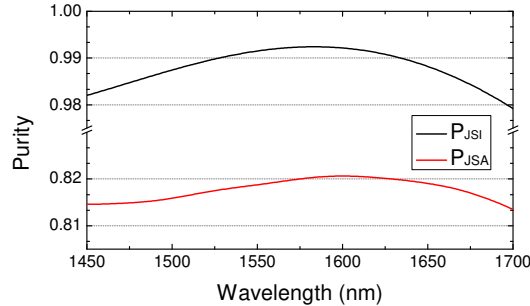


Fig. 2. Numerical simulation of the P_{JSI} and the P_{JSA} as functions of the wavelength.

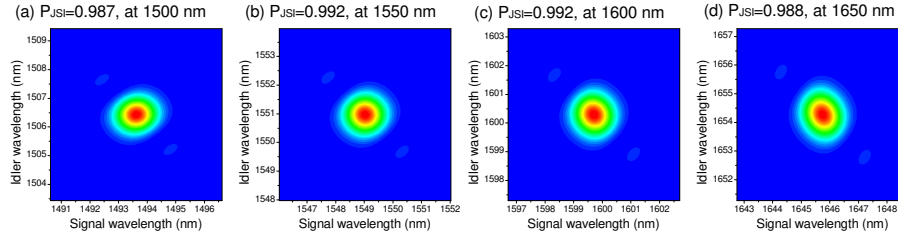


Fig. 3. Numerical simulation of the joint spectral intensity (JSI) at 1500 nm, 1550 nm, 1600 nm and 1650 nm.

for P_{JSI} and P_{JSA} are slightly different. It is noteworthy that the P_{JSI} and P_{JSA} can be kept between 0.983 and 0.993, and 0.815 and 0.821, respectively, from 1460 nm to 1675 nm. The P_{JSA} is smaller than the P_{JSI} , mainly caused by the side lobes in the phase matching amplitude $\phi(\omega_s, \omega_i)$. The P_{JSI} and P_{JSA} are relatively low in the regions around 1450 nm and 1700 nm. This is because the same bandwidth of the pump is used for all the wavelengths, but this bandwidth is optimum only for 1584 nm. If the bandwidth of the pump is optimized for 1450 nm or 1700 nm, we can also achieve a higher values for those regions. Figure 3(a-d) shows several examples of the JSI at 1500 nm, 1550 nm, 1600 nm, 1650 nm, respectively.

4. Experiment and results

The experimental setup is shown in Fig. 4. Picosecond laser pulses (temporal duration ~ 2 ps, central wavelength was tunable from 700 nm to 1000 nm) from a mode-locked Titanium sapphire laser (Coherent, Mira900) were used as the pump source for the SPDC. Pump pulses with power of 50 mW passed through a 30-mm-long PPKTP crystal with a poling period of $46.1 \mu\text{m}$ for type-II SPDC. The temperature was maintained at 32°C for the PPKTP crystal. The down-converted photons, i.e., the signal (vertically polarized) and the idler (horizontally polarized) were separated by a polarizing beam splitter (PBS) and collected into two single-mode fibers (SMF). Then the photons were filtered by two bandpass filters (BPFs, Optoquest), which had a filter function of Gaussian shape with an FWHM of 0.56 nm and a tunable central wavelength from 1560 nm to 1620 nm. Finally, all the collected photons were sent to two InGaAs avalanche photodiode (APD) detectors (ID210, idQuantique) connected to a coincidence counter (Ortec 9353).

To measure the JSI of the photon pairs, we scanned the central wavelength of the BPF1 and BPF2, and recorded the coincidence counts. BPF1 and BPF2 were moved in 0.1 nm per step and 60 by 60 steps in all. The coincidence counts were accumulated for 10 seconds for each point. With the pump wavelength set at 782.5 nm, 792 nm and 807.5 nm, we measured the JSI at 1565 nm, 1584 nm and 1615 nm, respectively.

The measured P_{JSI} were 0.989, 0.983 and 0.958, respectively, as shown in Fig. 5. The maximum coincidence counts rate decreased from 1075 cps at 1565 nm to 281 cps at 1615 nm,

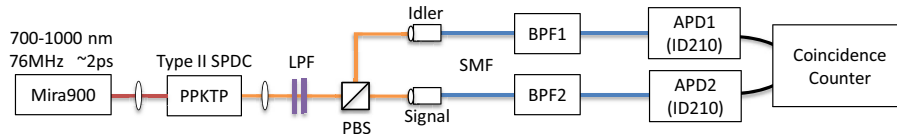


Fig. 4. The experimental setup. LPF (long-wave pass filter), PBS (polarizing beam splitter), SMF (single mode fiber), BPF (bandpass filter), APD (avalanche photodiodes).

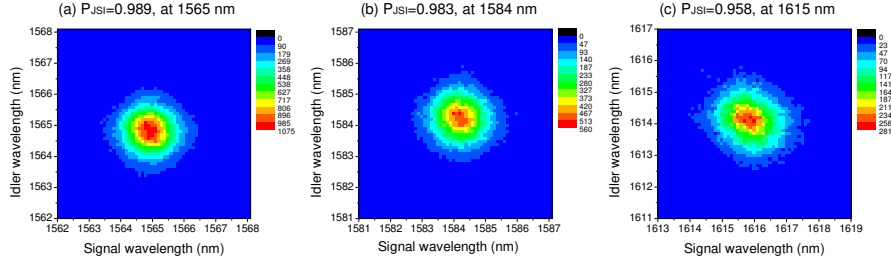


Fig. 5. Experimentally measured joint spectral intensity (JSI) at 1565 nm, 1584 nm and 1615 nm.

	Theoretical P_{JSI}	Convolved P_{JSI}	Experimental P_{JSI}	The difference
1565 nm	0.992	0.995	0.989	0.006
1584 nm	0.992	0.995	0.983	0.012
1615 nm	0.991	0.995	0.958	0.037

Table 1. Comparison of the theoretical, convolved and experimental P_{JSI} .

due to the decrease of the quantum efficiency of the APDs. As depicted in Fig. 2, the theoretical P_{JSI} for 1565 nm, 1584 nm and 1615 nm, were 0.992, 0.992 and 0.991, respectively. In the simulation of the theoretical P_{JSI} , we assumed that the bandwidth of two BPFs was narrow enough. However, in experiment the bandwidth of our BPFs (0.56 nm) was comparable to the bandwidth of the signal and idler (1.1 nm). So, it was necessary to consider the convolution effect of the two BPFs. We repeated the simulation with the real filter function and obtained the convolved P_{JSI} as 0.995, 0.995 and 0.995. The three measured P_{JSI} were very close to these convolved values, as shown in Tab. 1. The small disparities may have been caused by the dark counts in the APDs, or small differences in the BPFs.

It was noteworthy to compare the theoretically expected bandwidth and experimentally measured one. The measured spectrum was a convolution of the original spectrum and the filter function of the BPFs. The BPFs had a filter function of Gaussian shape with an FWHM of 0.56 nm, while the spectra of the signal and idler were also in a Gaussian shape. Thus we can calculate their convolution as $\text{FWHM}_{\text{con}} = \sqrt{0.56^2 + \text{FWHM}_{\text{the}}^2}$, where FWHM_{the} was the theoretical calculated FWHM of the original JSI. The experimentally measured FWHM_{exp} can be obtained from the marginal distribution of the data in Fig. 5. We compared the theoretical bandwidth and the experimentally measured bandwidth in Tab. 2. The convolved FWHMs were consistent with the measured ones. The small difference may arise from that the FWHM of pump laser was slightly different from the optimal FWHM in the simulation. In addition, the FWHM of the pump laser and the FWHM of the two BPFs were slightly wavelength-dependent.

5. Discussion and future

We need to clarify that purity of joint spectral intensity, P_{JSI} , is different from the traditional definition of spectral purity p , or P_{JSA} . There is no information on phase of the two-photon wave packet in JSI. Any phase would reduce the purity of the heralded single photons by introducing temporal correlations. Thus, we cannot directly obtain purity of the heralded single photons

	Theoretical	Convolved	Experimental	The
	FWHM_{the}	$\sqrt{0.56^2 + \text{FWHM}_{\text{the}}^2}$	FWHM_{exp}	difference
1565 nm signal	1.09 nm	1.23 nm	1.38 nm	0.15 nm
1565 nm idler	1.13 nm	1.26 nm	1.32 nm	0.06 nm
1584 nm signal	1.12 nm	1.25 nm	1.45 nm	0.20 nm
1584 nm idler	1.12 nm	1.25 nm	1.40 nm	0.15 nm
1615 nm signal	1.17 nm	1.30 nm	1.56 nm	0.26 nm
1615 nm idler	1.10 nm	1.23 nm	1.43 nm	0.20 nm

Table 2. Comparison of the convolved bandwidth and the experimentally measured bandwidth.

from JSI. As shown in Fig. 2, P_{JSA} is usually smaller than P_{JSI} , due to the side lobes in the JSA. However, the detrimental effect of the side lobes is not severe, according to the previous experiments. Several groups have reported high-visibility interference between the signal and idler photons from such PPKTP crystals, e.g., visibility has achieved 94% in [8] and 98% in [10]. Especially, the interference visibility was 95% for both PPKTP crystal and custom-poled crystal in [15].

To reduce the effect of side lobes in JSA, a new method of engineering the nonlinearity profile of the poled crystals has been proposed recently [15]. With this method, the phase matching amplitude can be tailored to approximate a Gaussian function. Therefore, the side lobes can be significantly suppressed and the P_{JSA} can be improved from 0.81 to 0.99 at 1576 nm [15]. They used higher-order poling to modulate the crystal. In this process, the material property of KTP was not changed. Therefore, in principle, widely tunable photon sources with higher purity could be generated with such custom-poled crystal. However, this method had the drawbacks of smaller effective nonlinearity and thus relatively lower photon pair rate [15] compared to the traditional PPKTP crystals. Alternatively, the purity can be improved by using a wide-band BPF to filter out the side lobes, but this method slightly decreases the count rate.

This spectrally pure photon source can be easily transformed into an entangled photon source by adding two calcite prisms as displacers [8, 16] or setting it into a Sagnac loop configuration [17, 18]. This photon source can be used for pulsed two-mode squeezed state generation by combining the signal and idler in the degenerate condition [19]. Another possible application for this photon source is wavelength-multiplexing based multiparty quantum communication system. If this PPKTP crystal is pumped by a laser frequency comb, e.g., with wavelengths distributed from 730 nm to 835 nm, we can generate serial pure photons distributed from 1460 nm to 1675 nm. These photons can be used for a wavelength-multiplexed system, which is one step for practical multiparty quantum communication systems.

The classical broadly tunable laser source have showed a tremendous impact in many and diverse fields of science and technology [1]. As the quantum counterpart of classical broadly tunable laser source, our widely tunable single photon source also has the potential to play an important role in quantum information and communication systems, when the wavelength tunability are necessary.

6. Summary

In summary, we have demonstrated the generation of widely tunable and highly pure photons from PPKTP crystal. In the theoretical simulation, we found the wavelength can be tuned from 1460 nm to 1675 nm, with P_{JSI} over 0.98 and P_{JSA} over 0.81. In experiment, we measured

the JSI at 1565 nm, 1584 nm and 1565 nm, and achieved P_{JSI} of 0.989, 0.983 and 0.958, respectively. This result was well consistent with our theoretical simulation. We also discussed the future application of this source.

Acknowledgments

The authors are grateful to M. Yabuno, P. G. Evans and T. Gerrits for helpful discussions. This work was supported by the Founding Program for World-Leading Innovative R&D on Science and Technology (FIRST).